Received: 2 May 2026 | Revised: 14 July 2026 | Accepted: 4 August 2026 | Published online: 24 August 2026

RESEARCH ARTICLE

Medinformatics
2026, Vol. 00(00) 1–13
DOI: 10.47852/bonviewMEDIN620210279

BON VIEW PUBLISHING

Mutational Landscape and Regulatory Network Analysis of TP53 and FOXA1 in Prostate Cancer

Shrijee Lakshkar[1,†], Pratha Tiwari[1,†], Heenal Bhatt[2], Vipin Ranga[3], Narendra Kumar Sharma[1,*] and Tikam Chand Dakal[4,*]

[1] *Department of Bioscience and Biotechnology, Banasthali Vidyapith, India*

[2] *Department of Biotechnology, Central University of Rajasthan, India*

[3] *Department of Biotechnology, Graphic Era (Deemed to be University), India*

[4] *Department of Biotechnology, Mohanlal Sukhadia University, India*

Abstract: Prostate cancer is a major global health burden. According to GLOBOCAN 2022 estimates, it accounts for nearly 396,792 deaths and 1,466,680 cases annually. Despite advances in immunotherapy, hormone therapy, radiation, chemotherapy, and surgery, improved biomarkers for early detection and targeted treatment remain urgently needed. In this study, cancer genomics data from cBioPortal were analyzed to identify key gene mutations associated with prostate cancer progression. Examination of 12,741 non-overlapping samples across 28 studies revealed diverse mutation frequencies among major driver genes. Among these, TP53 and FOXA1 showed the highest numbers of somatic mutations, at 3101 (frequency 25.6%) and 1386 (frequency 11.4%), respectively, with mutation hotspots concentrated in the p53 DNA-binding and FOXA1 forkhead domains. Missense mutations were the predominant alteration type, particularly in TP53, where they may disrupt tumor suppressor activity. FOXA1 mutations, observed in primary and metastatic castration-resistant prostate cancer, were associated with aggressive disease phenotypes and potential therapeutic resistance. Survival analysis revealed that TP53 mutations were significantly associated with poorer overall survival, whereas FOXA1 mutation status was not. Clinical analysis revealed higher nonsynonymous tumor mutational burden in TP53- and FOXA1-mutant tumors than in their wild-type counterparts. Protein–protein interactions between MDM2 and EP300 with TP53 and between GATA3 and FOXA1 highlighted their roles in transcriptional regulation and prostate cancer biology. Collectively, these findings highlight TP53 and FOXA1 as promising biomarkers and potential therapeutic targets in prostate cancer.

Keywords: prostate cancer, genomic profiling, mutations, TP53, FOXA1

1. Introduction

Prostate cancer is a specific type of cancer that develops in the prostate gland. While certain types of cancers spread quickly to other parts of the body, prostate cancer is localized, and it usually develops slowly. According to the GLOBOCAN 2022 estimates, approximately 1,466,680 new cases of prostate cancer and 396,792 deaths were reported worldwide in 2022 [1]. The main risk factors include age, family history, occupational exposure, diet, gut microbiome dysbiosis, genetic mutations, inflammation, and cellular damage. Symptoms of metastasized cancer include blood in the urine, bone discomfort, and difficulty urinating. Digital rectal examinations and prostate-specific antigen blood tests are two screening methods that can aid in the early detection of prostate cancer [2]. Some of the potential therapeutic options are immunotherapy, hormone therapy, radiation therapy, chemotherapy, surgery, and active monitoring.

Prostate cancer is classified into four stages: early-stage (stages I and II), locally advanced (stage III), and advanced (stage IV) [3]. Early-stage prostate cancer is typically localized to the prostate gland, whereas locally advanced prostate cancer extends to nearby tissues. Advanced or metastatic prostate cancer spreads to distant sites, including the lymph nodes, bones, liver, and lungs [4]. A number of issues are associated with cancer: medical problems such as tumor growth and metastasis, side effects from treatment such as erectile dysfunction, urinary incontinence, fatigue and bowel complications, and issues related to the progression and recurrence of the cancer [5, 6]. Several challenges are associated with prostate cancer, such as the psychological effects, decision-making, quality of life, and practical and financial

***Corresponding authors:** Narendra Kumar Sharma, Department of Bioscience and Biotechnology, Banasthali Vidyapith, India. Email: narendrakumarsharma@banasthali.in and Tikam Chand Dakal, Department of Biotechnology, Mohanlal Sukhadia University, India. Email: tc.dakal@mlsu.ac.in

†Shrijee Lakshkar and Pratha Tiwari contributed equally to this work

concerns [7]. These include stress management, sadness, anxiety, and fear. Other major problems include navigating complex treatment options, understanding medical information, and managing uncertainty about prognosis and outcomes [8].

In comparison to other cancers, prostate cancer has a lower mortality rate and a higher incidence rate, making it the second most diagnosed cancer in men worldwide [9]. Incidence rates are influenced by a number of variables, including age, genetics, diet and lifestyle [10]. Survival rates are high when it is detected early, with five-year relative survival exceeding 70% worldwide. Prostate cancer mortality and incidence are also influenced by lifestyle variables, age, race, and family history [11]. Active surveillance, surgery, radiation therapy, hormone therapy, chemotherapy, and immunotherapy are among the available treatment options for prostate cancer. Adopting a healthy lifestyle, including abstaining from alcohol and tobacco, maintaining a balanced diet, and engaging in regular physical activity, may further support disease management [12].

Genetic testing plays a crucial role in prostate cancer by identifying mutations in genes associated with disease risk and progression [12]. Biomarker-based assays analyze DNA from tissue or blood samples to detect specific genetic alterations and can be used to examine gene panels such as PTEN, TP53, FOXA1, BRCA1, and BRCA2 [13, 14]. In addition, next-generation sequencing enables analysis of large genomic regions or entire genomes to identify mutations that influence disease susceptibility and clinical outcomes [15]. Liquid biopsy approaches, including circulating tumor DNA, allow the detection of genetic mutations from tumor cells in a minimally invasive manner [16]. In clinical practice, biomarkers are used to stratify patients, guide therapeutic decisions, and monitor treatment response [13]. Furthermore, they are essential for understanding the genetic basis of prostate cancer, identifying novel therapeutic targets, and developing personalized treatment strategies [17].

The web-based platform cBioPortal provides visualization and analysis tools for large-scale cancer genomics datasets. It facilitates interactive study of gene expression, genetic changes, and clinical data to support cancer research [18]. In this portal, mutations in the TP53 gene, a key tumor suppressor, have been examined across a variety of cancer types [19]. Along with mutations, data on TP53 expression levels and the associations of mutations with clinical data have also been stored [20]. The platform includes visualization tools for showing mutation hotspots and their effects on protein structure and function. It also allows users to investigate the relationship between TP53 mutations and clinical indicators, such as survival rates and treatment response [21].

Although several studies have investigated TP53 and FOXA1 alterations in prostate cancer [22, 23]. Most have focused on individual aspects such as mutation frequency, expression changes, or specific molecular mechanisms. Comprehensive integrative analysis that combines large-scale genomic profiling, mutation hotspot characterization, structural interpretation of recurrent mutations, and regulatory network analysis across multiple prostate cancer cohorts remains limited. Therefore, in the present study, we systematically analyzed genomic data from 12,741 samples representing 28 prostate cancer studies available in cBioPortal to characterize the mutational landscape of TP53 and FOXA1. Furthermore, we examined mutation distributions, the relationship between mutations and mRNA expression levels, survival and clinical analyses, the structural consequences of recurrent hotspot mutations through protein–DNA complex analysis, and protein–protein interaction (PPI) networks to obtain a comprehensive understanding of the biological and clinical significance of these genes in prostate cancer. This integrative approach provides additional insights into the molecular mechanisms underlying prostate cancer progression and highlights TP53 and FOXA1 as potential biomarkers and therapeutic targets.

2. Methods and Materials

2.1. Study design

The aim of this study was to comprehensively characterize the mutational landscape of prostate cancer using genomic datasets available in cBioPortal and to identify key recurrently mutated genes associated with disease progression [24, 25]. Following the initial genome-wide mutation profiling, TP53 and FOXA1 were selected for detailed investigation because they possess higher mutation frequencies and represent biologically complementary regulators of prostate cancer. After visiting the cBioPortal website (https://www.cbioportal.org/), the "Prostate" option under "Quick select" was selected to get the detailed summary of datasets related to prostate cancer. This study was conducted on a dataset comprising 12,741 samples from 28 studies. The dataset was accessed on April 20, 2026, and studies with overlapping data were excluded from further bioinformatics analysis. The detailed description of the studies used, including study names and sample numbers, is provided in Table 1.

Table 1. Description of datasets and studies available at the cBioPortal platform

S. No.	Data description	Study center	Sample numbers
1	Prostate cancer	The German Cancer Research Center (Deutsches Krebsforschungszentrum, Dkfz)	324
2	Prostate cancer	Memorial Sloan Kettering Cancer Centre (MSK)	2260
3	Prostate cancer	Memorial Sloan Kettering Cancer Centre (MSK)	18
4	Prostate cancer brain metastases	University of Bern	168
5	Prostate cancer MDA PCa PDX	MD Anderson Cancer Center	88
6	Metastatic prostate cancer	NA	123
7	Metastatic prostate adenocarcinoma	Michigan Center for Translational Pathology	121
8	Metastatic prostate adenocarcinoma	The SU2C–Prostate Cancer Foundation (PCF) dream team	444
9	Metastatic prostate cancer	The SU2C–Prostate Cancer Foundation (PCF) dream team	150

(*Continued*)

Table 1. (*Continued*)

S. No.	Data description	Study center	Sample numbers
10	Metastatic castration-sensitive prostate cancer	Memorial Sloan Kettering Cancer Centre (MSK)	424
11	Neuroendocrine prostate cancer	Multi-institute	114
12	Prostate adenocarcinoma	Board/Cornell	82
13	Prostate adenocarcinoma	Board/Cornell	123
14	Prostate adenocarcinoma	The Canadian Prostate Cancer Genome Network (CPC-GENE)	477
15	Prostate adenocarcinoma	Fred Hutch Cancer Centre	176
16	Prostate adenocarcinoma	Memorial Sloan Kettering Cancer Centre (MSK)	240
17	Prostate adenocarcinoma	Memorial Sloan Kettering Cancer Centre (MSK)	1417
18	Prostate adenocarcinoma	Memorial Sloan Kettering Cancer Centre (MSK)	1465
19	Prostate adenocarcinoma	Memorial Sloan Kettering Cancer Centre (MSK)	104
20	Prostate adenocarcinoma	Memorial Sloan Kettering Cancer Centre (MSK)	1013
21	Prostate adenocarcinoma	SMMU	65
22	Prostate adenocarcinoma	The Cancer Genome Atlas, TCGA	494
23	Prostate adenocarcinoma organoids	Memorial Sloan Kettering Cancer Centre (MSK)	12
24	Prostate cancer	Memorial Sloan Kettering Cancer Centre (MSK)	504
25	Prostate cancer	Memorial Sloan Kettering Cancer Centre (MSK)	47
26	Race differences in prostate cancer	Memorial Sloan Kettering Cancer Centre (MSK)	2069
27	Prostate adenocarcinoma	Memorial Sloan Kettering Cancer Centre (MSK)	120
28	Prostate cancer-Isocitrate dehydrogenase (IDH) driver mutant cohort	Memorial Sloan Kettering Cancer Centre (MSK), 2024	99
		Total number of samples	12,741

2.2. Analysis of genetic mutations and their relation to the expression levels of TP53 and FOXA1

"Explore Selected Studies" was selected to obtain a detailed summary of different types of prostate cancer and their corresponding sample counts. Among the 12,741 samples, a specific prostate adenocarcinoma subtype (11,960 samples from 11,725 patients) was selected to assess alteration frequency, mutated genes, and copy-number variations in genes associated with prostate tumors [24, 26]. The "Mutated Genes" module provides a comprehensive list of all mutated genes, along with their mutation frequencies and the number of samples in which each gene is mutated. The "Plots" module was utilized to examine the mutation type, mutation count, and the fraction of the genome altered associated with TP53 and FOXA1. The correlation of clinical attribution provides information on TP53 and FOXA1 protein amino acid mutations, the positions of those amino acids, somatic mutation frequencies, 3D cancer hotspots, and oncoKB information. The "Quick Search" option was selected to examine the relationship between different mutation types and expression levels of TP53 and FOXA1. Under the "Plots" option, "mRNA vs mut type" was selected to visualize the major mutation types for each selected gene across different samples, along with their corresponding distributions of mRNA expression levels. For survival and clinical analysis, the "Comparison/Survival" option was selected.

2.3. PPI network construction

The PPI network of the protein under study was predicted using the STRING database version 12.0 (http://string-db.org), an online resource containing information on both experimentally verified and literature-reported protein interactions [27]. The "Protein by name" module of the STRING database was used to evaluate PPI network characteristics, including the number of nodes, the number of edges, and the expected number of edges. A high confidence score (0.7) and the maximum cutoff for the number of interacting proteins were selected in the advanced settings. Enrichment analysis of the TP53 and FOXA1-interacting proteins was conducted by clicking the "Analysis" option.

2.4. Structural analysis of mutated TP53 and FOXA1 proteins

The three-dimensional structures of human TP53–DNA (PDB ID: 2AC0, resolution 1.80 Å) and human FOXA1–DNA (PDB ID: 7VOX, resolution 2.10 Å) complexes were obtained from the Protein Data Bank [28]. The structures were visualized, and amino acids were replaced with the mutated ones using the PyMOL v3.1.0 tool (https://pymol.org/2/). Figures of the complexes were prepared in PyMOL.

2.5. Molecular dynamics simulations of wild-type and mutated TP53–DNA and FOXA1–DNA complexes and binding free energy calculations

Both the wild-type and mutated TP53–DNA and FOXA1–DNA complexes were evaluated for structural stability using the AMBER99SB force field in the GROMACS v2025.4 package [29]. The protein in a dodecahedral box was solvated with TIP3P water molecules. Neutralization of the solvated system was performed using Na^+ and Cl^- ions to achieve a final solvent concentration of 0.15 M. Steric clashes and unfavorable bond angles were removed by performing energy minimization

on the system. Furthermore, sequential 1 ns NVT and 1 ns NPT equilibration simulations were performed to stabilize the system before the production MD simulation. The Particle-mesh Ewald method was used with a cutoff distance of 10 Å to compute long-range electrostatic interactions. Molecular dynamics (MD) simulation runs of 100 ns each were performed. Simulation coordinates were recorded at 20 ps intervals, and the resulting trajectories were analyzed for root-mean-square deviation (RMSD) and root-mean-square fluctuation (RMSF) using GROMACS. A total of 500 frames were extracted to calculate the binding free energy (ΔG_bind) between the proteins (both wild-type and mutant) and their interacting DNA molecule using the Generalized Born method implemented in gmx_MMPBSA v1.5.0.3 [30]. All figures were generated using in-house Python scripts.

3. Results

3.1. Mutation of TP53 and FOXA1

Datasets related to prostate cancer in cBioPortal include observations from 12,741 non-overlapping samples across 28 studies. Of these, 11,960 samples representing 11,725 patients were selected for further analysis by focusing on the prostate adenocarcinoma subtype, which accounts for 98.4% of the total samples. Mutation profiles of genes from 11,960 samples revealed varying numbers of prostate adenocarcinoma-specific mutations. In decreasing order of the percentage of samples, the top ten highly mutated genes are listed in Table 2. It showed the number of mutations, the number of samples, and the percentage of samples in which one or more genes were found mutated.

Use of the cBioPortal platform to examine TP53 and FOXA1 mutational profiles across cancer types revealed notable findings. In patients with prostate adenocarcinoma, the percentage of samples with a somatic TP53 mutation frequency was 25.6%, with a total of 3101 mutations in 2961 samples. For FOXA1, the somatic mutation frequency was 11.4%, with a total of 1386 mutations in 1317 samples. Figure 1(A) illustrates the distribution of mutations across the major functional domains of TP53, including the transactivation motif, DNA-binding domain, and tetramerization motif. Among 11,725 patients, the mutation landscape showed domain-specific patterns, with a substantial proportion of alterations occurring in functionally critical regions. A total of 2184 driver mutations were identified in TP53 across the analyzed prostate cancer samples. Among these, missense mutations were the predominant alteration type, accounting for 1940 mutations (88.8%), followed by splice-site mutations (196; 8.9%), and in-frame mutations (48; 2.1%). The DNA-binding domain (positions 95 to 288 amino acids) showed a high mutation burden. These were primarily missense mutations leading to amino acid substitutions such as R248 to Q/W/L in 70 patients, R273 to C/H/L/P in 97 patients, and R175 to H/G/L in 53 patients. Additionally, 52 unique nonsense mutations were observed in TP53 in 160 samples comprising 139 patients. These mutations include variants such as R213*, Q165*, R196*, E298*, Q52*, G266*, and R342*, with R213* being the most frequently observed amino acid mutation, identified in 39 patients, followed by Q165* (16 patients), R196* and E298* (15 patients each), and Q52*, G266*, and R342* (13 patients each). Overall, the DNA-binding domain emerges as a major mutation hotspot, consistent with its central role in TP53 function.

Figure 1(B) presents mutation profiling across the functional domains of FOXA1, namely, forkhead N-terminal (17–169 aa), forkhead (170–265 aa), and HNF C-terminal (397–461 aa). Among these, the forkhead domain showed the highest mutation frequency. A total of 809 driver mutations were identified in FOXA1 across the analyzed prostate cancer samples. Unlike TP53, in-frame mutations were the predominant alteration type in FOXA1, accounting for 468 mutations (57.8%), and missense mutations were the second most common with 340 mutations (42%). Some of the prominent in-frame mutations include F254_N256delinsY, F254V, F254_E255del, F254_G257delinsC/R/RKF, E255Tfs*62, and F254_P297del. In addition, 21 patients displayed in-frame mutations at position 253, including M253K, M253R, M253V, M253T, M253_N256del, M253_Y259del, or insertion variants,

Table 2. Top 10 mutated genes in prostate adenocarcinoma subtype

Gene	Gene details	No. of mutations	No. of samples	Frequency (%)
TP53	A tumor suppressor gene, most frequently mutated gene in cancer	3101	2961	25.6
TTN	Encodes a large abundant protein of striated muscles	572	420	13.2
SPOP	A tumor suppressor gene, targets androgen receptor (AR), SRC3 and BRD4 for degradation in prostate cancer	1361	1339	11.7
FOXA1	A transcription factor, the third most frequently mutated gene in prostate cancer	1386	1317	11.4
MUC16	Transmembrane glycoprotein implicated in cancer progression and widely used as a tumor biomarker	372	308	9.7
PTEN	A lipid and protein phosphatase, is one of the most frequently mutated genes in cancer	822	769	6.7
KMT2C	A tumor suppressor and histone methyltransferase, is altered in various solid and hematologic malignancies	867	741	6.5
SYNE1	Nuclear envelope protein involved in maintaining nuclear architecture and cytoskeletal organization	246	202	6.4
APC	A tumor suppressor involved in WNT signaling	776	720	6.2
KMT2D	A tumor suppressor and histone methyltransferase, one of the most frequently mutated genes in cancer	843	696	6.1

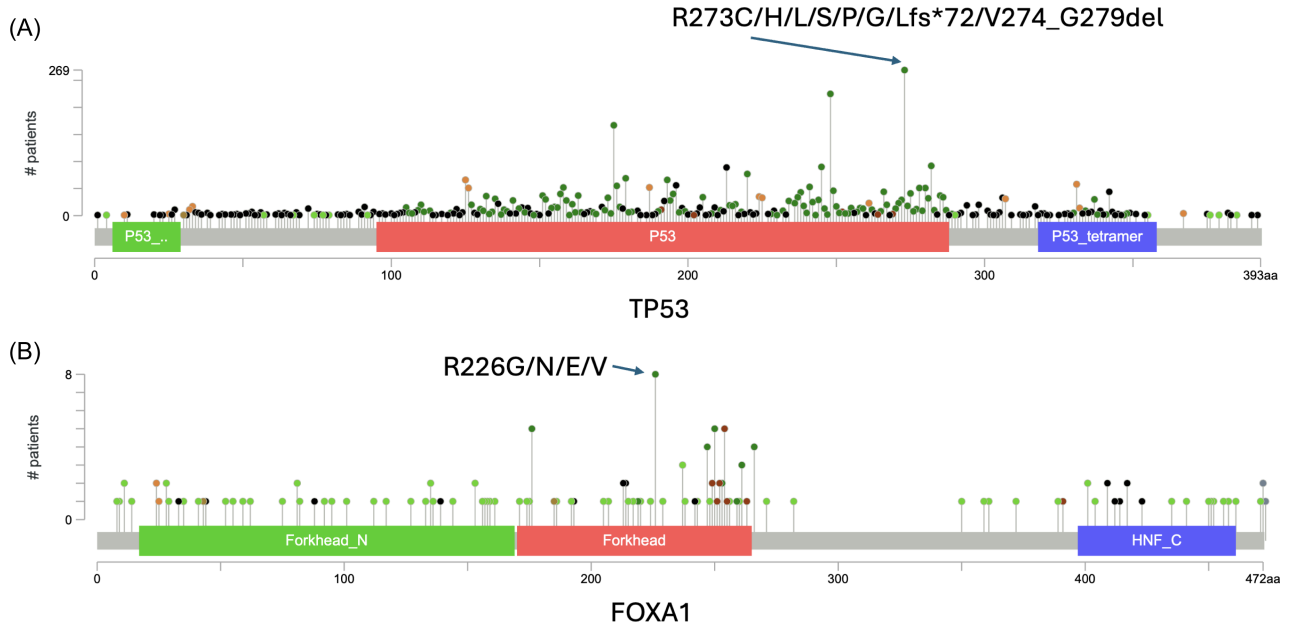

Figure 1. The top two highly mutated proteins in prostate cancer. (A) Lollipop plot showing the distribution and frequency of TP53 mutations across the protein sequence and annotated functional domains. (B) Lollipop plot showing the distribution and frequency of FOXA1 mutations across the protein sequence and annotated functional domains. The height of each lollipop represents the number of affected patients. Mutation classes are color-coded as green for missense, black for truncating, brown for in-frame, orange for splice, and purple for fusion alterations, with darker and lighter shades representing driver mutations and variants of uncertain significance (VUS), respectively

and frameshift mutations such as M253Ifs64 and M253Nfs63. These mutations are predominantly localized within the forkhead domain and its adjacent regions, indicating that this region is particularly susceptible to structural alterations. Similar to TP53, arginine residues in FOXA1 were frequently affected by missense mutations, including R219S/C in 29 patients and R261G/C/H/S/P in 30 patients, which are located within the forkhead domain. Overall, both TP53 and FOXA1 showed domain-specific clustering of mutations, highlighting critical functional regions that are frequently altered in disease contexts.

3.2. Association between TP53 mutation types and mRNA expression

To better understand the relationship between TP53 mutations and mRNA expression in prostate cancer, TP53 mRNA expression levels were analyzed across different mutation categories, including truncating, splice-site, missense, and in-frame mutations (Figure 2(A)). Missense mutations were the predominant alteration type, comprising 2185 samples, and were primarily classified as driver mutations, with a small number of variants of unknown significance. Samples containing missense mutations generally exhibited higher TP53 mRNA expression levels (median: 10.8) than those with truncating mutations (median: 8.8) or splice-site mutations (median: 9.2). In-frame mutations were less frequent (75 samples) but were associated with relatively high TP53 expression levels, with a median of approximately 10.9. Overall, these findings indicate mutation-type-specific variation in TP53 mRNA expression, with missense and in-frame mutations associated with relatively higher expression levels than truncating and splice-site mutations.

Kaplan–Meier analysis of 4686 patients, including 1307 with TP53-mutant tumors and 3379 with TP53 wild-type tumors, revealed a highly significant difference in overall survival between the two groups (log-rank $p < 10^{-10}$; $q < 10^{-10}$) (Figure 2(B)). Patients with TP53 mutations showed poorer overall survival than those with TP53 wild-type tumors, with the mutant group exhibiting an earlier and more pronounced decline in survival probability. These findings indicate that TP53 mutation status is significantly associated with unfavorable overall survival in prostate cancer. Survival analysis revealed no significant difference in overall survival between patients with FOXA1-mutant and FOXA1 wild-type tumors ($p = 0.378$), although the FOXA1-mutant group exhibited a shorter estimated median overall survival (73.7 months) than the wild-type group (82.2 months). This finding is consistent with Hwang et al. [31], who reported that FOXA1 alterations did not significantly influence survival when considered collectively.

Clinical outcome analysis of nonsynonymous tumor mutational burden (TMB) showed significantly higher values in the mutant group than in the wild-type group, with $p < 1 \times 10^{-10}$ and $q < 1 \times 10^{-10}$ (Figure 2(C)). The mutant group showed a median TMB of 2 (interquartile range 0.98–3.83; maximum 8.12), whereas the wild-type group showed a lower median TMB of 1.11 (interquartile range 0.37–2.59; maximum 5.94).

3.3. Association between FOXA1 mutation types and mRNA expression

Similar to TP53, mRNA expression levels of FOXA1 were analyzed across mutation categories, including truncating, splice-site, missense, and in-frame mutations (Figure 3(A)). Among these, missense mutations were the predominant type of alteration in 93 samples and showed highly heterogeneous expression with a mean of 9.06 and a median of 10.43. Truncating mutations were identified in 17 samples with a mean expression of 10.92 and a median of 12.80. In-frame mutations detected in 14 samples were associated with the highest FOXA1 expression, with

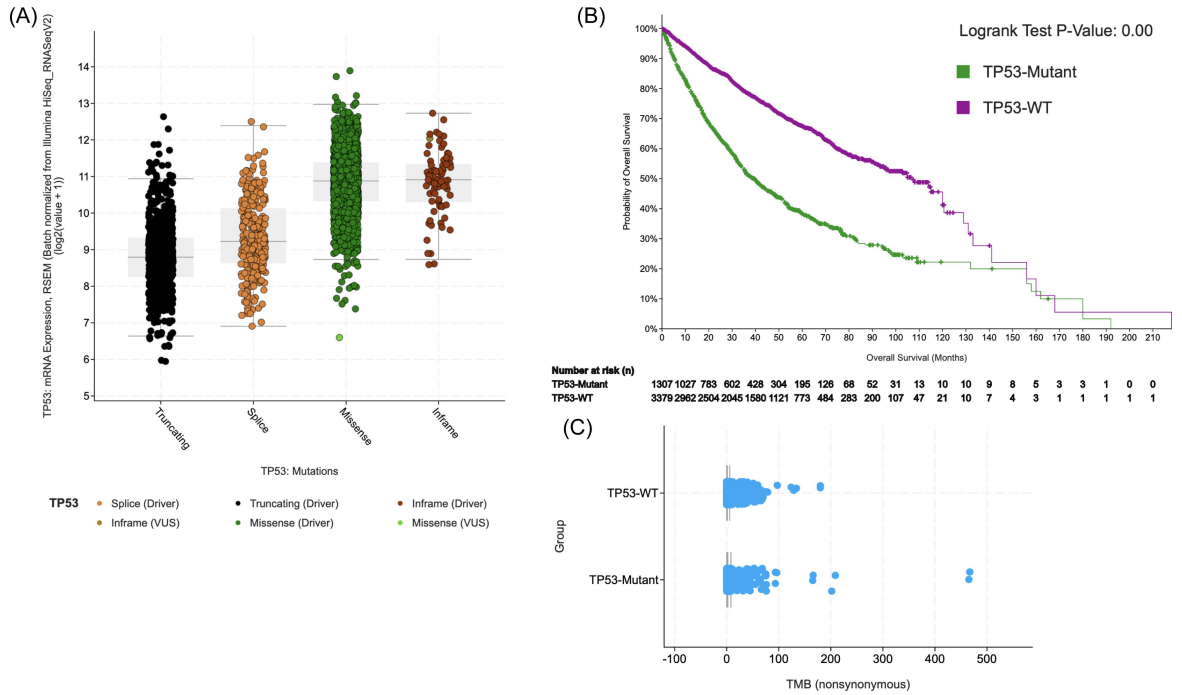

Figure 2. Association of TP53 mutations with mRNA expression, overall survival, and tumor mutational burden. (A) Distribution of TP53 mRNA expression across tumors harboring truncating, splice, missense, and in-frame mutations. Individual points represent samples, with colors indicating the corresponding mutation classes and their driver or variant of uncertain significance (VUS) annotations. (B) Kaplan–Meier overall survival curves comparing patients with TP53-mutant tumors shown in green and TP53-WT tumors shown in purple; the number-at-risk table is presented below the survival curves. (C) Distribution of nonsynonymous tumor mutational burden TMB in TP53-mutant and TP53-WT groups, with individual points representing samples in each group

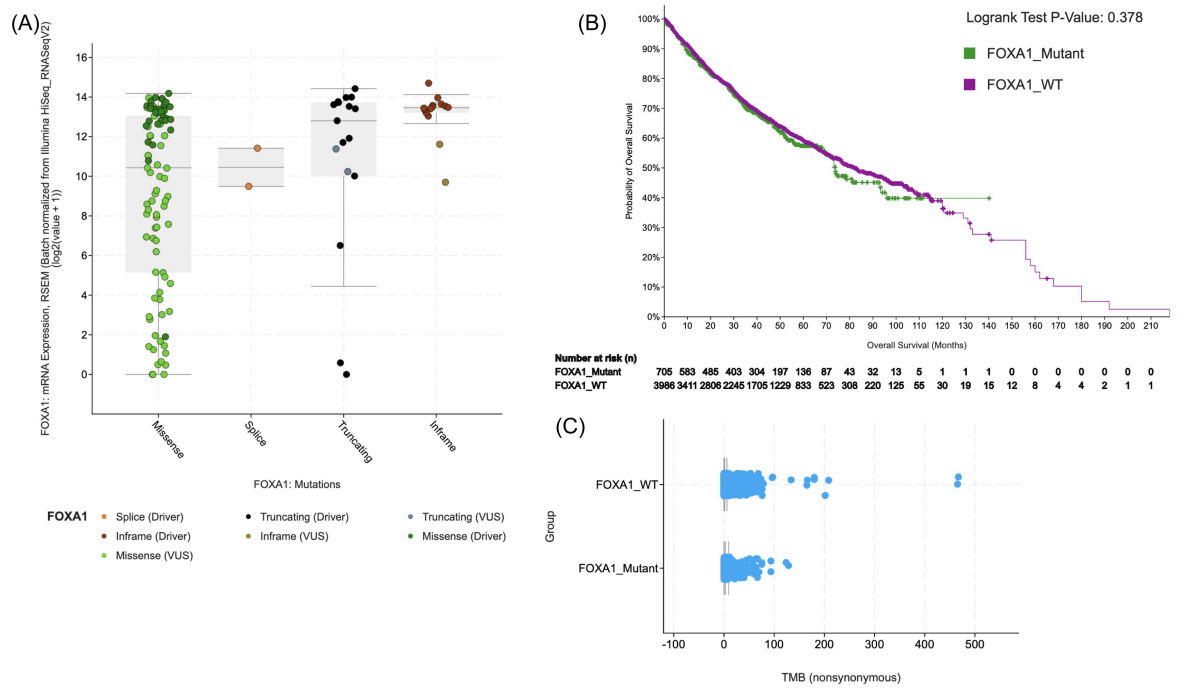

Figure 3. Association of FOXA1 mutations with mRNA expression, overall survival, and tumor mutational burden. (A) Distribution of FOXA1 mRNA expression across tumors harboring truncating, splice, missense, and in-frame mutations. Individual points represent samples, with colors indicating the corresponding mutation classes and their driver or variant of uncertain significance (VUS) annotations. (B) Kaplan–Meier overall survival curves comparing patients with FOXA1-mutant tumors shown in green and FOXA1-WT tumors shown in purple; the number-at-risk table is presented below the survival curves. (C) Distribution of nonsynonymous tumor mutational burden TMB in FOXA1-mutant and FOXA1-WT groups, with individual points representing samples in each group

a mean of 13.16 and a median of 13.46. Splice mutations were observed in only two samples and showed a mean and median expression of 10.45. Overall, in-frame mutations were associated with the highest FOXA1 mRNA expression, whereas missense mutations displayed the greatest expression heterogeneity across samples.

Kaplan–Meier survival analysis of FOXA1 showed no significant difference in overall survival between patients with FOXA1-mutant and FOXA1-WT tumors (log-rank p-value = 0.378) (Figure 3(B)). The estimated median overall survival was 73.7 months in the FOXA1-mutant group and 82.2 months in the FOXA1-WT group. Although FOXA1-mutant tumors showed shorter median overall survival, the difference was not statistically significant. This analysis indicates that FOXA1 mutation status alone was not associated with overall survival in the analyzed cohort.

Clinical outcome analysis of nonsynonymous TMB identified higher values in the FOXA1-mutant group than in the FOXA1-WT group (Figure 3(C)). The FOXA1-mutant group showed a median TMB of 2.59 (interquartile range, 0.97–4.32), compared with 1.30 (interquartile range, 0.50–2.70) in the FOXA1-WT group. The mean TMB was also higher in the FOXA1-mutant group than in the FOXA1-WT group, with values of 4.11 and 2.69, respectively. These findings indicate a greater overall nonsynonymous mutational burden in FOXA1-mutant tumors.

3.4. Arginine mutation reduces ionic interactions in TP53–DNA complexes

TP53 is a crucial tumor suppressor gene known for regulating cell division, repairing DNA damage, and initiating apoptosis in faulty cells. In prostate cancer, the aforementioned mutations in TP53 are critically affecting disease progression, metastasis, and therapy resistance. For the structural analysis, molecular interactions between TP53 and its DNA motif were inspected (PDB ID: 2AC0). The positively charged amino acid arginine at position 273 forms ionic interactions with the negatively charged phosphate backbone of the DNA molecule (Figure 4(A)). Loss of ionic interactions may disrupt the molecular interactions of TP53 with the DNA motif due to the replacement of charged arginine with a small and uncharged cysteine residue (Figure 4(B)). Visual inspection of mutations other than R273C revealed no interactions with DNA molecules and suggested they may be involved in maintaining structural integrity.

To examine this at the atomic level, both the wild-type and mutant TP53–DNA complexes were subjected to 100 ns MD simulations. Comparison of the RMSD and RMSF profiles indicated that the wild-type and R273C mutant TP53 proteins maintained overall structural stability throughout the simulation runs (Figures 4(C) and 4(D)). The wild-type TP53 protein showed average RMSD and RMSF values of 1.69 ± 0.33 Å and

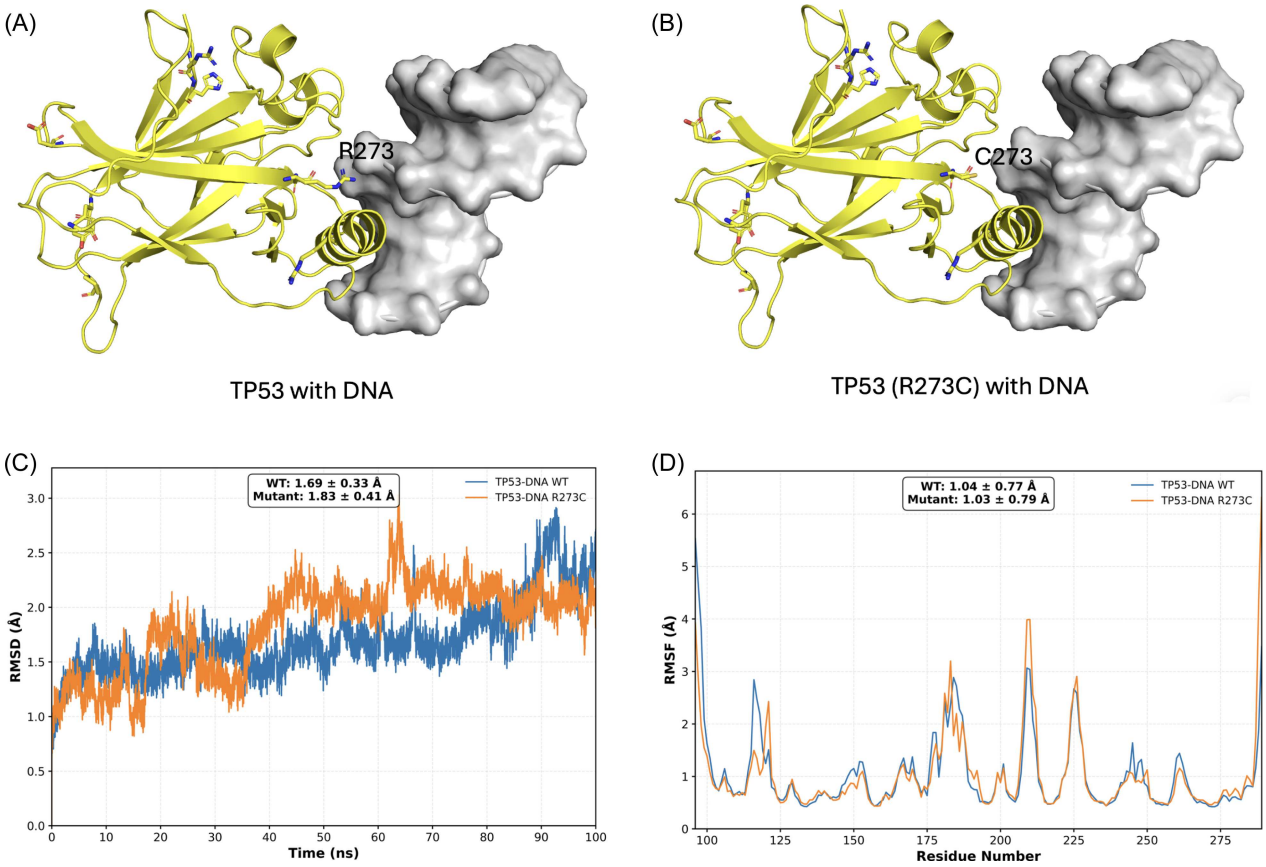

Figure 4. TP53 complex with DNA. (A) The wild-type form of TP53 in humans makes interactions with a double-stranded DNA motif. (B) The mutated form of TP53 (R273C) does not make hydrogen-bonding interactions with the DNA molecule because of its small size and non-charged nature. (C) Root-mean-square deviation (RMSD) profiles of the wild-type TP53–DNA complex shown in blue and the R273C mutant TP53–DNA complex shown in orange during the 100 ns molecular dynamics simulations. (D) Residue-wise root-mean-square fluctuation (RMSF) profiles of the wild-type TP53–DNA complex shown in blue and the R273C mutant TP53–DNA complex shown in orange

1.04 ± 0.77 Å, respectively. The R273C mutant showed corresponding average values of 1.83 ± 0.41 Å and 1.03 ± 0.79 Å. Despite their overall structural stability, differences in the dynamic behavior of the two complexes were observed during the simulations. Molecular Mechanics/Generalized Born Surface Area (MM/GBSA) analysis further revealed a significant difference in the estimated binding free energy between the wild-type and R273C mutant TP53–DNA complexes. The wild-type complex exhibited an average binding free energy of −61.36 ± 8.18 kcal mol^{-1}, whereas the R273C mutant complex showed −48.99 ± 9.56 kcal mol^{-1}. The less favorable binding free energy observed for the R273C mutant complex indicated that the mutation weakened the interaction between TP53 and DNA.

3.5. Arginine mutation reduces ionic interactions in FOXA1–DNA complexes

The FOXA1 transcription factor usually binds to nucleosomes to allow the opening of compacted chromatin. Mapping of the mutated amino acids (R219S and R219C) to the DNA-bound three-dimensional structure of FOXA1 (PDB ID: 7VOX) showed that R219 is the most critical residue, making direct hydrogen-bonding interactions with the DNA-binding site (Figure 5(A)). Mutations of arginine to serine (Figure 5(B)) or cysteine (Figure 5(C)) at position 219 have the potential to disrupt molecular interactions due to their small, polar side chains and inability to form direct interactions with the DNA molecule. To investigate the effects of the R219S and R219C mutations on the DNA-binding stability of FOXA1, the wild-type (WT) and mutant FOXA1–DNA complexes were subjected to 100 ns MD simulations. Comparison of the RMSD and RMSF profiles indicated that the wild-type and mutant FOXA1 proteins maintained overall structural stability throughout the simulation runs (Figures 5(D) and 5(E)). The wild-type FOXA1 protein showed average RMSD and RMSF values of 1.81 ± 0.59 Å and 1.33 ± 1.06 Å, respectively. The R219S mutant exhibited corresponding values of 1.72 ± 0.29 Å and 1.02 ± 0.69 Å, whereas the R219C mutant showed average RMSD and RMSF values of 2.00 ± 0.42 Å and 1.10 ± 1.06 Å, respectively. As expected, a significant difference was observed in the estimated binding free energy of the wild-type FOXA1–DNA complex (−103.07 ± 17.87 kcal mol^{-1}) compared with the R219S (−84.47 ± 11.72 kcal mol^{-1}) and R219C (−96.26 ± 13.74 kcal mol^{-1}) mutant complexes. Both FOXA1 mutations reduced the number of ionic interactions between the positively charged arginine residue and the negatively charged phosphate groups of the DNA molecule.

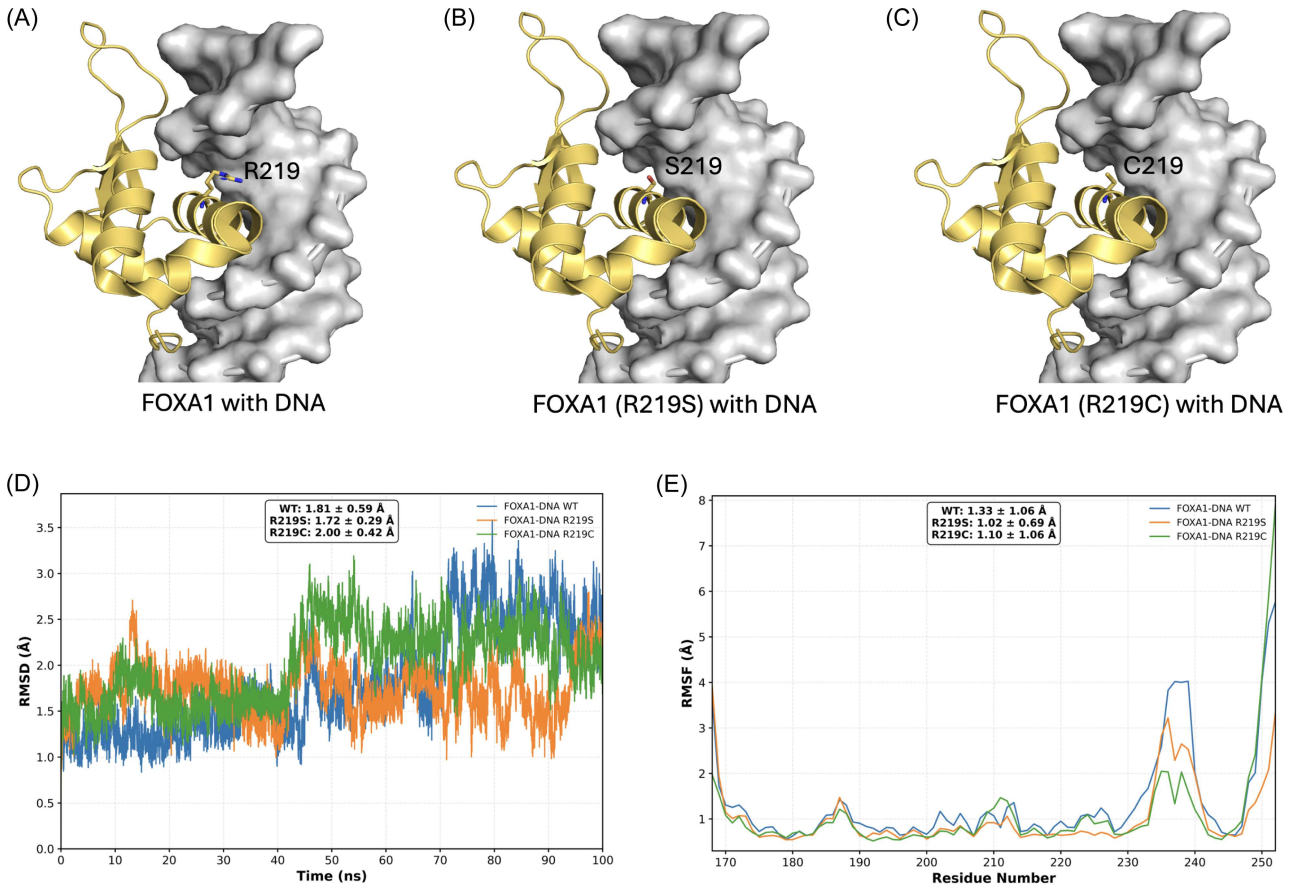

Figure 5. FOXA1 complex with DNA. (A) The wild-type form of FOXA1 in humans makes interactions with a double-stranded DNA motif. (B) The mutated form of FOXA1 (R219S) does not make hydrogen-bonding interactions with the DNA molecule because of its small size and non-charged nature. (C) The mutated form of FOXA1 (R219C) does not make hydrogen-bonding interactions with the DNA molecule because of its small size and non-charged nature. (D) RMSD profiles of the wild-type FOXA1–DNA complex shown in blue, the R219S mutant shown in orange, and the R219C mutant shown in green during the 100 ns molecular dynamics simulations. (E) RMSF profiles of the wild-type FOXA1–DNA complex shown in blue and the R219S and R219C mutants shown in orange and green, respectively

3.6. Protein–protein interaction network and functional enrichment analyses of TP53

PPI network analysis of TP53 and its associated proteins revealed a highly interconnected network comprising 51 nodes and 374 edges, with an average node degree of 14.7 and an average local clustering coefficient of 0.691 (Figure 6(A)). The observed number of interactions resulted in a highly significant PPI enrichment p-value of $< 1.0 \times 10^{-16}$. This enrichment indicated that the proteins within the network were functionally connected and likely participated in shared biological processes rather than representing a random set of proteins.

Functional enrichment analysis in the STRING database further revealed a strong association between the TP53 interaction network and DNA damage responses, apoptosis, transcriptional regulation, and p53-mediated signaling. Among the most significantly enriched Gene Ontology biological processes were regulation of signal transduction by p53 class mediator (GO:1901796), involving 16 of 105 proteins with an enrichment strength of 4.98 and a false discovery rate (FDR) of 1.11×10^{-20}; response to gamma radiation (GO:0010332), involving 12 of 55 proteins with an enrichment strength of 4.66 and FDR of 5.42×10^{-17}; and intrinsic apoptotic signaling in response to DNA damage (GO:0008630), involving 13 of 75 proteins with an enrichment strength of 4.52 and FDR of 2.20×10^{-17} (Figure 6(B)).

Gene Ontology molecular function analysis showed enrichment for p53 binding (GO:0002039), involving 15 of 70 proteins with an enrichment score of 5.44 and an FDR of 1.22×10^{-20}. Other enriched molecular functions included RNA polymerase II-specific DNA-binding transcription factor binding (GO:0061629), DNA-binding transcription factor binding (GO:0140297), transcription factor binding (GO:0008134), and ubiquitin protein ligase binding (GO:0031625). Cellular component enrichment indicated that network proteins were predominantly associated with nuclear regulatory structures, including the promyelocytic leukemia (PML) body, transcription repressor complex, transcription regulator complex, nuclear body, and replication fork. Pathway enrichment analysis further supported the central role of the TP53-associated network in cancer-related mechanisms. Kyoto Encyclopedia of Genes and Genomes (KEGG) analysis identified the p53 signaling pathway (hsa04115) as one of the most strongly enriched pathways, involving 14 of 72 proteins with an enrichment strength of 5.22 and an FDR of 3.69×10^{-20}. Significant enrichment was also observed for cell-cycle regulation (hsa04110), prostate cancer (hsa05215), and other cancer types.

3.7. Protein–protein interaction network and functional enrichment analyses of FOXA1

PPI network analysis of FOXA1 and its associated proteins revealed a highly interconnected network comprising 51 nodes and 318 edges, with an average node degree of 12.5 and an average local clustering coefficient of 0.713 (Figure 7(A)). The observed number of interactions resulted in a highly significant PPI enrichment p-value of $< 1.0 \times 10^{-16}$. Functional enrichment analysis revealed that the FOXA1-associated network was predominantly linked to epithelial differentiation, developmental regulation, miRNA transcription, and sex differentiation. Among the most significantly enriched Gene Ontology biological processes were columnar/cuboidal epithelial cell differentiation (GO:0002065), involving 10 of 105 proteins with an enrichment strength of 2.69 and an FDR of 6.32×10^{-11}; hepaticobiliary system development (GO:0061008), involving 11 of 134 proteins with an enrichment strength of 2.68 and an FDR of 1.76×10^{-11}; and gland development (GO:0048732), involving 19 of 419 proteins with an enrichment strength of 2.62 and an FDR of 2.57×10^{-16}.

Gene Ontology molecular function analysis showed strong enrichment for transcription coregulator binding (GO:0001221), involving 13 of 114 proteins with an enrichment strength of 3.69 and an FDR of 1.82×10^{-15}. Other significantly enriched

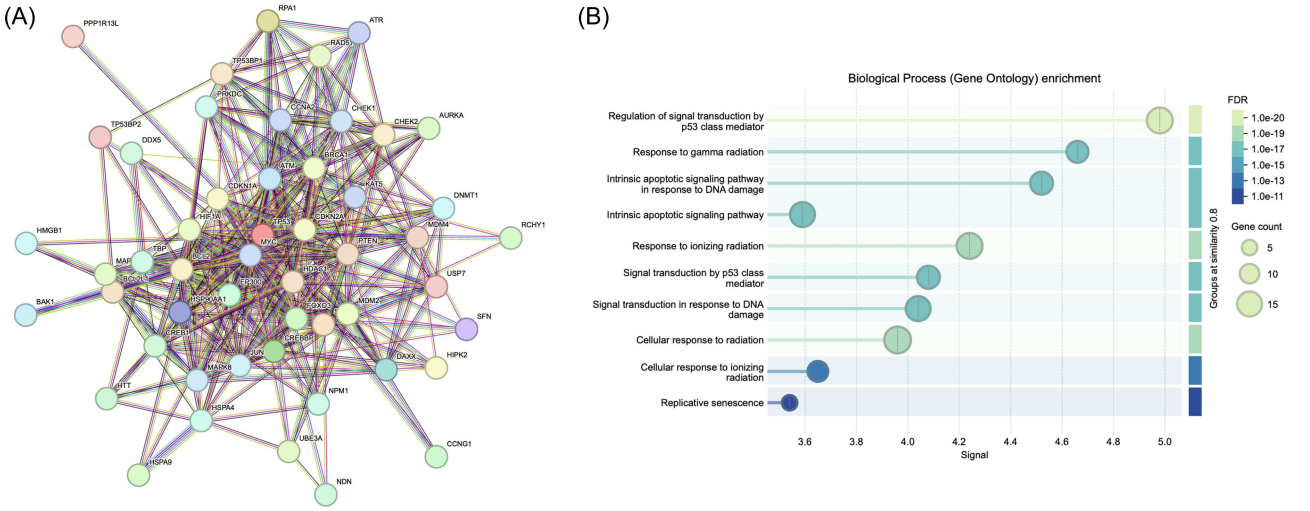

Figure 6. Protein–protein interaction network and GO enrichment analysis of TP53-associated proteins. (A) Nodes represent proteins, whereas edges indicate known or predicted functional associations among them. The network showed interactions with proteins involved in DNA damage response (e.g., ATM, ATR, BRCA1, CHEK1, CHEK2, RAD51, and TP53BP1), regulators of cell-cycle progression (e.g., CDKN1A, CDKN2A, CCNA2, and AURKA), apoptosis-related proteins (e.g., BAK1, BCL2, and BCL2L1), and transcriptional co-regulators (e.g., EP300, CREBBP, MYC, JUN, and TBP). (B) Bubble plot showing the top enriched GO biological processes identified for the TP53 interaction network. Bubble size is proportional to the number of proteins assigned to each GO term, while color intensity represents FDR values. The highest-ranked biological processes include regulation of p53-mediated signal transduction, cellular responses to DNA damage and ionizing radiation, intrinsic apoptotic signaling, and replicative senescence.

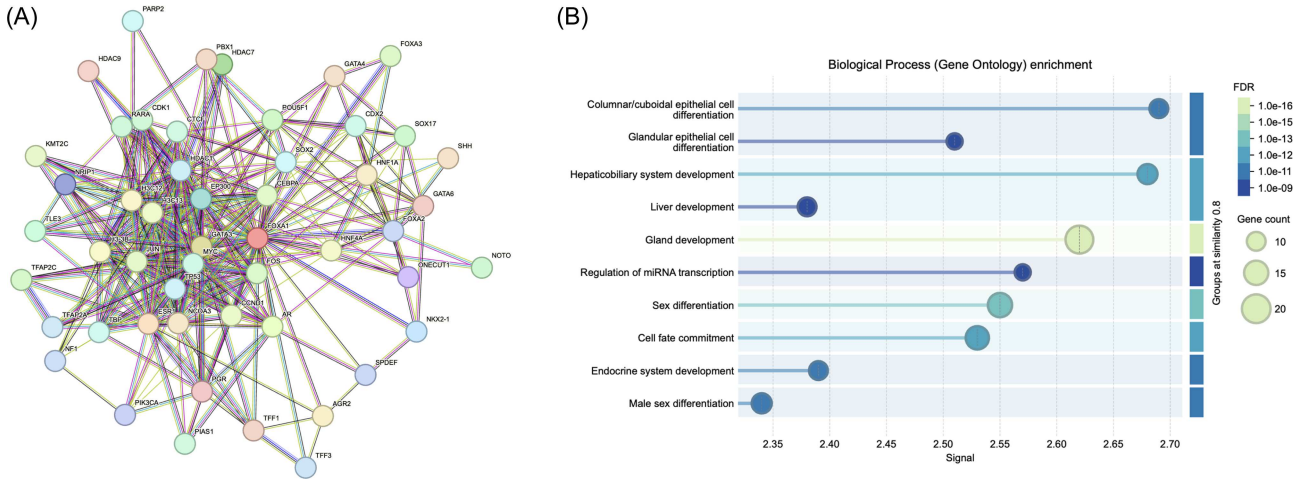

Figure 7. Protein–protein interaction network and GO enrichment analysis of FOXA1-associated proteins. (A) PPI network of FOXA1 and its interacting proteins generated using the STRING database. Nodes represent proteins, whereas edges indicate known or predicted functional associations derived from multiple evidence sources. The network shows interactions between FOXA1 and key transcription factors (e.g., TP53, CDX2, SOX2, MYC, JUN, and PBX1), chromatin regulators (e.g., EP300, HDAC1, HDAC7, and HDAC9), hormone receptor signaling components (e.g., AR, ESR1, PGR, PIAS1, TFF1, TFF3, and AGR2) and cancer-associated proteins (e.g., TP53, MYC, PIK3CA, PARP2, CDK1, and KMT2C). (B) GO biological process enrichment analysis of the FOXA1-associated protein network. The bubble plot shows the top significantly enriched biological processes. The x-axis represents the enrichment signal; bubble size corresponds to the number of genes associated with each GO term, and bubble color indicates FDR values. The most significantly enriched biological processes include columnar and glandular epithelial cell differentiation, hepatobiliary system, liver and gland development, regulation of miRNA transcription, and cell fate commitment.

functions included transcription factor binding (GO:0008134), DNA-binding transcription factor binding (GO:0140297), transcription coactivator binding (GO:0001223), and RNA polymerase II-specific DNA-binding transcription factor binding (GO:0061629) (Figure 7(B)).

Pathway enrichment analysis further showed the involvement of the FOXA1 network in hormone-responsive and cancer-associated signaling. KEGG pathways included thyroid hormone signaling (hsa04919), breast cancer (hsa05224), viral carcinogenesis (hsa05203), and endocrine resistance (hsa01522). FOXA1 showed strong interactions with several biologically relevant transcriptional regulators. Interaction with androgen receptor (AR) highlights its role in androgen signaling and prostate cancer biology. Similarly, interaction with estrogen receptor 1 (ESR1) supports a role for FOXA1 in hormone receptor-mediated transcriptional regulation. The network also revealed interaction with GATA3, which is a transcriptional activator implicated in epithelial differentiation and developmental regulation. Collectively, these findings suggest that FOXA1 functions as a central regulatory hub coordinating transcriptional and hormonal pathways relevant to prostate cancer progression.

4. Discussion

Prostate cancer is one of the most prevalent malignancies in men, accounting for approximately 396,792 deaths annually and more than 1.47 million cases worldwide in 2022 [1]. Current therapeutic strategies include immunotherapy, hormone therapy, radiation therapy, chemotherapy, surgery, and active surveillance; however, the search for robust biomarkers for early diagnosis and targeted intervention remains a major priority for improving patient outcomes [32, 33].

In the present study, mutation profiles were examined across 28 prostate cancer studies, encompassing 12,741 samples, to investigate the mutational landscape of major driver genes associated with prostate cancer progression. Frequent mutations were identified in several genes, including TP53, FOXA1, SPOP, KMT2C, KMT2D, PTEN, TTN, CDK12, MUC16, and SYNE1, ranked according to the number of mutations. Among these, TP53 and FOXA1 were prioritized due to their high mutation frequencies and functional relevance to prostate tumorigenesis [22, 34]. Mutation profiling revealed that alterations in TP53 and FOXA1 are concentrated within their critical functional domains, particularly the p53 DNA-binding domain and the forkhead domain, respectively, suggesting these regions as major mutational hotspots [22]. Consistent with previous reports, missense mutations represented the predominant mutation type in both genes [35, 36]. In TP53, these mutations may contribute not only to loss of tumor suppressor activity but also to gain-of-function properties that promote malignancy [37]. Likewise, FOXA1 mutations, reported in approximately 4% of primary prostate cancers and enriched in metastatic castration-resistant disease (~10%), are associated with aggressive tumor phenotypes and possible resistance to current therapies [34, 38].

Associations between genomic alterations and expression patterns suggested that TP53 and FOXA1 mutations may influence prostate cancer progression through distinct but interconnected mechanisms [39, 40]. Consistent with our analysis, higher TP53 expression levels were observed in samples with missense mutations than in those with truncating or splice mutations [19]. Unlike TP53, FOXA1 showed higher expression levels in tumors with truncating mutations than in those harboring missense mutations. This distinct expression pattern may reflect mutation-specific regulatory effects, consistent with previous studies demonstrating that structurally distinct FOXA1 alterations show heterogeneous functional consequences [41]. The relationship between truncating mutations and FOXA1 expression in prostate cancer presents an apparent paradox: although these

mutations produce truncated proteins, certain variants can confer hyperactive gain-of-function properties that enhance downstream oncogenic transcriptional activity [40].

Mapping mutations onto the three-dimensional structure of protein–DNA complexes highlighted the role of the positively charged arginine residue in interacting with DNA bases and negatively charged phosphate groups. The mutated forms of TP53 and FOXA1 (arginine residues mutated to small, nonpolar amino acids) may disrupt molecular interactions due to the loss of ionic interactions formed by the arginine residues.

KEGG enrichment analysis identified involvement of TP53 and its interacting proteins in various other pathways, such as prostate cancer, p53 signaling pathway, cell cycle, cellular senescence, and apoptosis. In human cancers, about 50% of tumors harbor mutations in TP53, which lead to uncontrolled cell proliferation, chemotherapy resistance, and poor prognosis. FOXA1 protein was also found to interact with prostate cancer-associated regulators such as AR and ESR1. Functional enrichment suggested that these interactions are linked to hormone receptor signaling and prostate developmental pathways. Given that FOXA1 facilitates chromatin accessibility for androgen and estrogen receptors, its mutational disruption may alter transcriptional programs involved in tumor suppression and oncogenesis [41]. Moreover, the association of FOXA1 expression with androgen and estrogen receptor signaling further supports its role in prostate cancer progression and prognosis [42].

Kaplan–Meier survival analysis showed that TP53 mutations were significantly associated with poorer overall survival in prostate cancer, with TP53-mutant tumors showing an earlier and more pronounced decline in survival probability than TP53 wild-type tumors. These findings are consistent with the study by Zhou et al. [19], who reported shorter median overall survival in patients with TP53-mutant tumors than in those with TP53 wild-type tumors (32.26 vs 75.2 months; $p < 0.0001$). Survival analysis of FOXA1 showed no significant difference in overall survival between patients with FOXA1-mutant and FOXA1 wild-type tumors ($p = 0.378$), although patients with FOXA1-mutant tumors had a shorter estimated median overall survival than those with wild-type tumors. Our observation is consistent with Hwang et al. [31], who reported that FOXA1 alterations, when analyzed collectively, were not significantly associated with survival. Although FOXA1 mutation status alone may have limited prognostic value, classification of FOXA1 alterations by specific mutation types or structural classes may provide more accurate prognostic information and further support the potential role of FOXA1 as a molecular biomarker in prostate cancer.

Comparison of the FOXA1 and TP53 interaction networks revealed distinct but potentially complementary functional patterns. The TP53-associated network was predominantly enriched in DNA damage response, apoptosis, cell-cycle regulation, ATM signaling, and p53-mediated stress responses. In contrast, the FOXA1-associated network was primarily enriched in transcriptional coregulation, chromatin organization, nuclear receptor signaling, and hormone-responsive pathways. Notably, the enrichment of the AR network in prostate cancer within the FOXA1 network provides a direct connection to prostate cancer-associated transcriptional regulation. Together, these findings suggest that alterations in TP53 and FOXA1 may affect different but biologically complementary regulatory systems in prostate cancer.

Despite the comprehensive analysis of multiple prostate cancer cohorts, this study has certain limitations. The findings are based exclusively on publicly available genomic datasets integrated within cBioPortal and were not independently validated using external patient cohorts or experimental approaches. Furthermore, variations in sequencing platforms, sample composition, and clinical characteristics among the included studies may have contributed to inter-study heterogeneity. Nevertheless, integrating data from 28 independent prostate cancer cohorts enabled the identification of recurrent mutation patterns and reduced the influence of study-specific bias. Future investigations incorporating independent clinical cohorts, transcriptomic and proteomic datasets, and functional experiments will be essential for validating the biological significance and clinical utility of the identified TP53 and FOXA1 mutation hotspots. Collectively, these findings highlight the significance of TP53 and FOXA1 mutations in prostate cancer biology and support their potential as biomarkers and therapeutic targets.

5. Conclusion

The present study provides comprehensive insights into the molecular landscape of TP53 and FOXA1 in prostate cancer, highlighting their mutational profiles, prognostic relevance, and functional interactions. Both genes appear to participate in diverse oncogenic processes and key regulatory pathways associated with prostate cancer progression. Differential expression patterns across multiple malignancies, including cervical, ovarian, and breast cancers, further suggest broader roles for these genes in hormone regulation and cancer-associated signaling pathways. Mutation profiling revealed recurrent alterations in TP53 and FOXA1, particularly within the p53 DNA-binding and forkhead domains, identifying these regions as major mutational hotspots. Missense mutations were the predominant mutation type in both genes, while truncating mutations in TP53 were associated with higher fractions of genome alteration and potential oncogenic consequences. PPI analysis of TP53 and FOXA1 revealed their involvement in central regulatory hubs and their connections to key prostate cancer-associated regulators, supporting their importance in disease-related molecular networks. Collectively, these findings emphasize the critical roles of TP53 and FOXA1 alterations in prostate cancer biology and support their potential utility as biomarkers for early detection and as candidates for personalized therapeutic strategies. Improved understanding of these molecular signatures may contribute to better prognostic assessment and more effective targeted interventions for prostate cancer patients.

Ethical Statement

This research involved only computational analyses and did not include experiments involving humans or animals. Therefore, ethical approval and informed consent were not required.

Conflicts of Interest

The authors declare that they have no conflicts of interest to this work.

Data Availability Statement

Data sharing is not applicable to this article as no new data were generated or analyzed during the current study.

Author Contribution Statement

Shrijee Lakshkar: Validation, Formal analysis, Investigation, Writing – original draft. **Pratha Tiwari:** Validation, Formal analysis, Investigation, Writing – original draft. **Heenal Bhatt:** Investigation, Writing – original draft. **Vipin Ranga:** Methodology,

Validation, Formal analysis, Investigation, Data curation, Writing – original draft, Writing – review & editing, Visualization. **Narendra Kumar Sharma:** Investigation, Writing – original draft, Writing – review & editing, Supervision. **Tikam Chand Dakal:** Conceptualization, Methodology, Validation, Formal analysis, Investigation, Data curation, Writing – original draft, Writing – review & editing, Visualization, Supervision, Project administration.

References

[1] Bray, F., Laversanne, M., Sung, H., Ferlay, J., Siegel, R. L., Soerjomataram, I., & Jemal, A. (2024). Global cancer statistics 2022: GLOBOCAN estimates of incidence and mortality worldwide for 36 cancers in 185 countries. *CA: A Cancer Journal for Clinicians*, *74*(3), 229–263. https://doi.org/10.3322/caac.21834

[2] Chung, Y., & Hong, S. K. (2025). Evaluating prostate cancer diagnostic methods: The role and relevance of digital rectal examination in modern era. *Investigative and Clinical Urology*, *66*(3), 181–187. https://doi.org/10.4111/icu.20240456

[3] Sekhoacha, M., Riet, K., Motloung, P., Gumenku, L., Adegoke, A., & Mashele, S. (2022). Prostate cancer review: Genetics, diagnosis, treatment options, and alternative approaches. *Molecules*, *27*(17), 5730. https://doi.org/10.3390/molecules27175730

[4] Roberts, M. J., Maurer, T., Perera, M., Eiber, M., Hope, T. A., Ost, P., & Fendler, W. P. (2023). Using PSMA imaging for prognostication in localized and advanced prostate cancer. *Nature Reviews Urology*, *20*(1), 23–47. https://doi.org/10.1038/s41585-022-00670-6

[5] Gandaglia, G., Leni, R., Bray, F., Fleshner, N., Freedland, S. J., Kibel, A., . . . , & La Vecchia, C. (2021). Epidemiology and prevention of prostate cancer. *European Urology Oncology*, *4*(6), 877–892. https://doi.org/10.1016/j.euo.2021.09.006

[6] Xiao, J., Zhang, M., & Wu, D. (2024). Side effects of prostate cancer therapies and potential management. *Journal of Biological Methods*, *11*(3), e99010018. https://doi.org/10.14440/jbm.2024.0019

[7] Xiang, J., Dai, L., Tan, L., Lv, D., Chen, Y., Tang, L., . . . , & Liu, X. (2025). Psychosocial experiences of prostate cancer survivors after treatment: A systematic review of qualitative studies. *Frontiers in Public Health*, *13*, 1625611. https://doi.org/10.3389/fpubh.2025.1625611

[8] Li, Y., Gillanders, D., & Finucane, A. (2025). Experience of uncertainty in prostate cancer: A qualitative study. *PLOS One*, *20*(10), e0334180. https://doi.org/10.1371/journal.pone.0334180

[9] Wang, L., Lu, B., He, M., Wang, Y., Wang, Z., & Du, L. (2022). Prostate cancer incidence and mortality: Global status and temporal trends in 89 countries from 2000 to 2019. *Frontiers in Public Health*, *10*, 811044. https://doi.org/10.3389/fpubh.2022.811044

[10] Bergengren, O., Pekala, K. R., Matsoukas, K., Fainberg, J., Mungovan, S. F., Bratt, O., . . . , & Carlsson, S. V. (2023). 2022 update on prostate cancer epidemiology and risk factors—A systematic review. *European Urology*, *84*(2), 191–206. https://doi.org/10.1016/j.eururo.2023.04.021

[11] Berenguer, C. V., Pereira, F., Câmara, J. S., & Pereira, J. A. M. (2023). Underlying features of prostate cancer—Statistics, risk factors, and emerging methods for its diagnosis. *Current Oncology*, *30*(2), 2300–2321. https://doi.org/10.3390/curroncol30020178

[12] de la Calle, C. M., Bhanji, Y., Pavlovich, C. P., & Isaacs, W. B. (2022). The role of genetic testing in prostate cancer screening, diagnosis, and treatment. *Current Opinion in Oncology*, *34*(3), 212–218. https://doi.org/10.1097/CCO.0000000000000823

[13] Eickelschulte, S., Riediger, A. L., Angeles, A. K., Janke, F., Duensing, S., Sültmann, H., & Görtz, M. (2022). Biomarkers for the detection and risk stratification of aggressive prostate cancer. *Cancers*, *14*(24), 6094. https://doi.org/10.3390/cancers14246094

[14] Miyahira, A. K., Hawley, J. E., Adelaiye-Ogala, R., Calais, J., Nappi, L., Parikh, R., . . . , & Soule, H. R. (2023). Exploring new frontiers in prostate cancer research: Report from the 2022 Coffey-Holden prostate cancer academy meeting. *The Prostate*, *83*(3), 207–226. https://doi.org/10.1002/pros.24461

[15] Chehade, C. H., Jo, Y., Gebrael, G., Tripathi, N., Sayegh, N., Chigarira, B., . . . , & Swami, U. (2024). Trends and disparities in next-generation sequencing in metastatic prostate and urothelial cancers. *JAMA Network Open*, *7*(7), e2423186. https://doi.org/10.1001/jamanetworkopen.2024.23186

[16] Garofoli, M., Maiorano, B. A., Bruno, G., Giordano, G., Falagario, U. G., Necchi, A., . . . , & Conteduca, V. (2025). Circulating tumor DNA: A new research frontier in urological oncology from localized to metastatic disease. *European Urology Oncology*, *8*(3), 805–817. https://doi.org/10.1016/j.euo.2024.11.008

[17] Davoudi, F., Moradi, A., Becker, T. M., Lock, J. G., Abbey, B., Fontanarosa, D., . . . , & Batra, J. (2023). Genomic and phenotypic biomarkers for precision medicine guidance in advanced prostate cancer. *Current Treatment Options in Oncology*, *24*(10), 1451–1471. https://doi.org/10.1007/s11864-023-01121-z

[18] Gazola, A. A., Lautert-Dutra, W., Archangelo, L. F., dos Reis, R. B. & Squire, J. A. (2024). Precision oncology platforms: Practical strategies for genomic database utilization in cancer treatment. *Molecular Cytogenetics*, *17*(1), 28. https://doi.org/10.1186/s13039-024-00698-w

[19] Zhou, J., Lai, Y., Peng, S., Tang, C., Chen, Y., Li, L., . . . , & Guo, Z. (2022). Comprehensive analysis of TP53 and SPOP mutations and their impact on survival in metastatic prostate cancer. *Frontiers in Oncology*, *12*, 957404. https://doi.org/10.3389/fonc.2022.957404

[20] Ren, S., Wei, G.-H., Liu, D., Wang, L., Hou, Y., Zhu, S., . . . , & Sun, Y. (2018). Whole-genome and transcriptome sequencing of prostate cancer identify new genetic alterations driving disease progression. *European Urology*, *73*(3), 322–339. https://doi.org/10.1016/j.eururo.2017.08.027

[21] Gao, J., Aksoy, B. A., Dogrusoz, U., Dresdner, G., Gross, B., Sumer, S. O., . . . , & Schultz, N. (2013). Integrative analysis of complex cancer genomics and clinical profiles using the cBioPortal. *Science Signaling*, *6*(269), pl1. https://doi.org/10.1126/scisignal.2004088

[22] Xu, X., Xie, L., Meng, L., Geng, S., Liu, J., Cao, X., . . . , & Xing, Z. (2022). Genetic features of TP53 mutation and its downstream FOXA1 in prostate cancer. *Bioscience Trends*, *16*(3), 221–229. https://doi.org/10.5582/bst.2022.01235

[23] Lehrer, S., & Rheinstein, P. (2026). FOXA1 alterations in prostate cancer: Expression, mutation classes, and copy number changes. *In Vivo*, *40*(1), 341–348. https://doi.org/10.21873/invivo.14197

[24] Cerami, E., Gao, J., Dogrusoz, U., Gross, B. E., Sumer, S. O., Aksoy, B. A., ..., & Schultz, N. (2012). The cBio cancer genomics portal: An open platform for exploring multidimensional cancer genomics data. *Cancer Discovery*, *2*(5), 401–404. https://doi.org/10.1158/2159-8290.CD-12-0095

[25] Wang, Y., Wang, J., Yan, K., Lin, J., Zheng, Z., & Bi, J. (2020). Identification of core genes associated with prostate cancer progression and outcome via bioinformatics analysis in multiple databases. *PeerJ*, *8*, e8786. https://doi.org/10.7717/peerj.8786

[26] Weinstein, J. N., Collisson, E. A., Mills, G. B., Mills Shaw, K. R., Ozenberger, B. A., Ellrott, K., ..., & Stuart, J. M. (2013). The Cancer Genome Atlas Pan-Cancer analysis project. *Nature Genetics*, *45*(10), 1113–1120. https://doi.org/10.1038/ng.2764

[27] Szklarczyk, D., Kirsch, R., Koutrouli, M., Nastou, K., Mehryary, F., Hachilif, R., ..., & von Mering, C. (2023). The STRING database in 2023: Protein-protein association networks and functional enrichment analyses for any sequenced genome of interest. *Nucleic Acids Research*, *51*(D1), D638–D646. https://doi.org/10.1093/nar/gkac1000

[28] Berman, H. M., Westbrook, J., Feng, Z., Gilliland, G., Bhat, T. N., Weissig, H., ..., & Bourne, P. E. (2000). The protein data bank. *Nucleic Acids Research*, *28*(1), 235–242. https://doi.org/10.1093/nar/28.1.235

[29] Lindorff-Larsen, K., Piana, S., Palmo, K., Maragakis, P., Klepeis, J. L., Dror, R. O., & Shaw, D. E. (2010). Improved side-chain torsion potentials for the Amber ff99SB protein force field. *Proteins*, *78*(8), 1950–1958. https://doi.org/10.1002/prot.22711

[30] Valdés-Tresanco, M. S., Valdés-Tresanco, M. E., Valiente, P. A., & Moreno, E. (2021). gmx_MMPBSA: A new tool to perform end-state free energy calculations with GROMACS. *Journal of Chemical Theory and Computation*, *17*(10), 6281–6291. https://doi.org/10.1021/acs.jctc.1c00645

[31] Hwang, J., Likasitwatanakul, P., Deshmukh, S. K., Wu, S., Kwon, J. J., Toye, E., ..., & Antonarakis, E. S. (2025). Structurally oriented classification of *FOXA1* alterations identifies prostate cancers with opposing clinical outcomes and distinct molecular and immunologic subtypes. *Clinical Cancer Research*, *31*(5), 936–948. https://doi.org/10.1158/1078-0432.CCR-24-3471

[32] Chen, J.-Y., Wang, P.-Y., Liu, M.-Z., Lyu, F., Ma, M.-W., Ren, X.-Y., & Gao, X.-S. (2023). Biomarkers for prostate cancer: From diagnosis to treatment. *Diagnostics*, *13*(21), 3350. https://doi.org/10.3390/diagnostics13213350

[33] Vakili, S., Beheshti, I., Barzegar Behrooz, A., Łos, M. J., Vitorino, R., & Ghavami, S. (2025). Transforming prostate cancer care: Innovations in diagnosis, treatment, and future directions. *International Journal of Molecular Sciences*, *26*(11), 5386. https://doi.org/10.3390/ijms26115386

[34] Dong, H.-Y., Ding, L., Zhou, T.-R., Yan, T., Li, J., & Liang, C. (2023). FOXA1 in prostate cancer. *Asian Journal of Andrology*, *25*(3), 287–295. https://doi.org/10.4103/aja202259

[35] Joerger, A. C., Stiewe, T., & Soussi, T. (2025). *TP53*: The unluckiest of genes? *Cell Death & Differentiation*, *32*(2), 219–224. https://doi.org/10.1038/s41418-024-01391-6

[36] Hwang, K. W., Yun, J. W., & Kim, H. S. (2023). Unveiling the molecular landscape of *FOXA1* mutant prostate cancer: Insights and prospects for targeted therapeutic strategies. *International Journal of Molecular Sciences*, *24*(21), 15823. https://doi.org/10.3390/ijms242115823

[37] Chen, X., Zhang, T., Su, W., Dou, Z., Zhao, D., Jin, X., ..., & Di, C. (2022). Mutant p53 in cancer: From molecular mechanism to therapeutic modulation. *Cell Death & Disease*, *13*(11), 974. https://doi.org/10.1038/s41419-022-05408-1

[38] Tam, K. J., Liu, L., Hsing, M., Dalal, K., Thaper, D., McConeghy, B., ..., & Ong, C. J. (2024). Clinically-observed FOXA1 mutations upregulate *SEMA3C* through transcriptional derepression in prostate cancer. *Scientific Reports*, *14*(1), 7082. https://doi.org/10.1038/s41598-024-57854-w

[39] Santos-Pereira, M., Pereira, S. C., Rebelo, I., Spadella, M. A., Oliveira, P. F., & Alves, M. G. (2023). Decoding the influence of obesity on prostate cancer and its transgenerational impact. *Nutrients*, *15*(23), 4858. https://doi.org/10.3390/nu15234858

[40] Parolia, A., Cieslik, M., Chu, S.-C., Xiao, L., Ouchi, T., Zhang, Y., ..., & Chinnaiyan, A. M. (2019). Distinct structural classes of activating FOXA1 alterations in advanced prostate cancer. *Nature*, *571*(7765), 413–418. https://doi.org/10.1038/s41586-019-1347-4

[41] Özturan, D., Morova, T., & Lack, N. A. (2022). Androgen receptor-mediated transcription in prostate cancer. *Cells*, *11*(5), 898. https://doi.org/10.3390/cells11050898

[42] Gao, S., Patten, N. D., & Cai, C. (2026). Alterations in AR-FOXA1 signaling in prostate cancer progression and therapeutic resistance. *Journal of the National Cancer Center*, *6*(1), 58–72. https://doi.org/10.1016/j.jncc.2025.05.003

How to Cite: Lakshkar, S., Tiwari, P., Bhatt, H., Ranga, V., Sharma, N. K., & Dakal, T. C. (2026). Mutational Landscape and Regulatory Network Analysis of TP53 and FOXA1 in Prostate Cancer. *Medinformatics*. https://doi.org/10.47852/bonviewMEDIN620210279